# Advances in Optics Photonics Spectroscopy & Applications XII

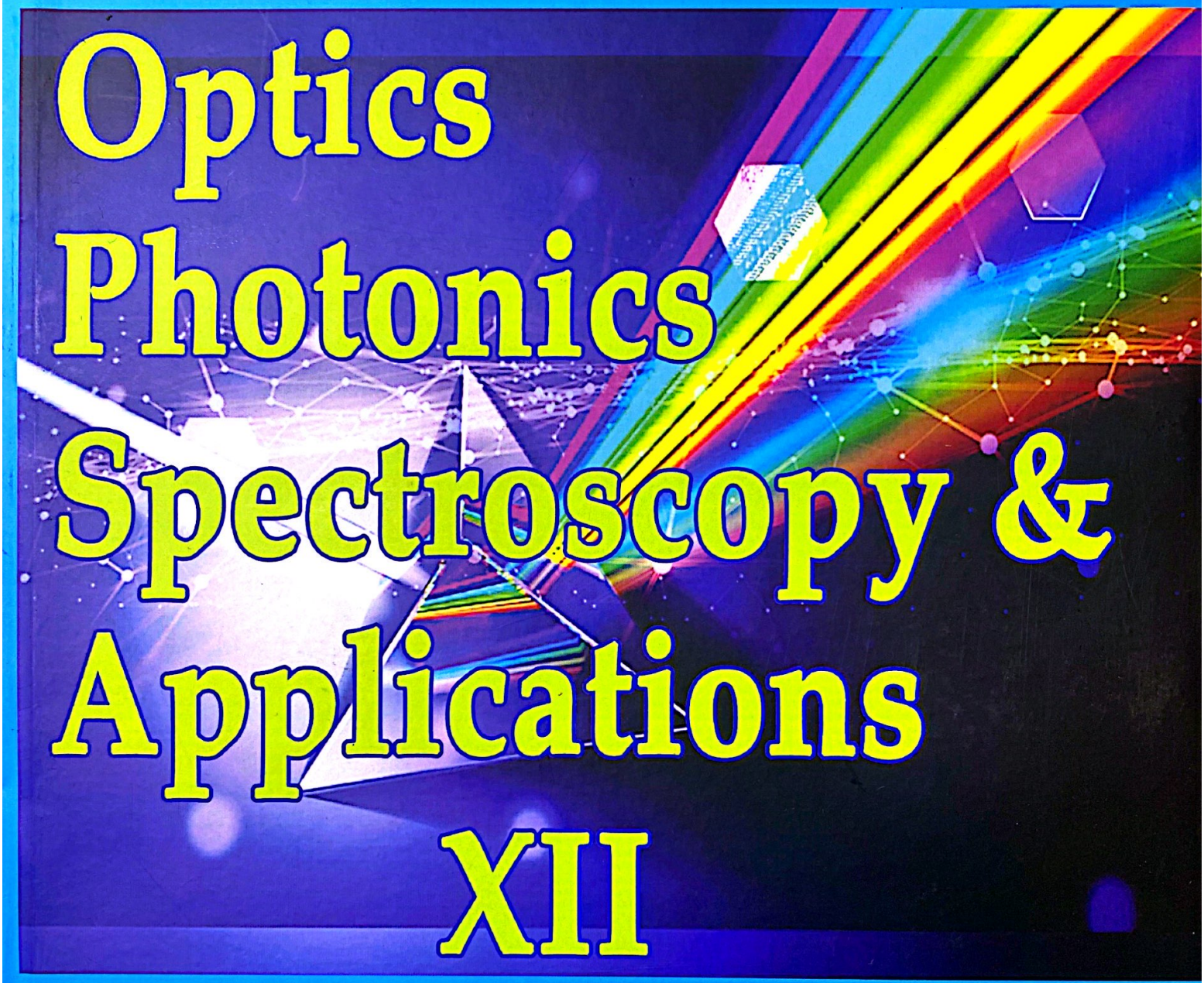

Philippe Brechignac, Yeung Lak Lee, Huynh Thanh Dat
N. Dai Hung, Valentin A. Orlovich, Nobuhiko Sarukura

Publishing House for Science and Technology

**PUBLISHING HOUSE FOR SCIENCE AND TECHNOLOGY**
A16, 18 Hoang Quoc Viet Road, Cau Giay, Ha Noi
Marketing & Distribution Department: **024.22149040**;
Editorial Department: **024.37917148**
Administration Support Department: **024.22149041**
Fax: **024.37910147**, Email: **nxb@vap.ac.vn;** Website: **www.vap.ac.vn**

# ADVANCES IN OPTICS PHOTONICS SPECTROSCOPY & APPLICATIONS XII

**Philippe Brechignac, Yeung Lak Lee, Huynh Thanh Dat, N. Dai Hung, Valentin A. Orlovich, Nobuhiko Sarukura**

***Responsible for Publishing***
*Director, Editor in Chief*
**PHAM THI HIEU**

| | |
|---|---|
| ***Editors:*** | **Ha Thi Thu Trang, Nguyen Thi Chien** |
| ***Computing Technique:*** | **Nguyen Truong Son** |
| ***Cover design:*** | **Nguyen Xuan Tu** |

**ISBN: 978-604-357-120-2**

Printing 150 copies, size 20.5×29.5cm, printed at An Thanh Company Limited.
Address: Van Con, Hoai Duc, Ha Noi.
Registered number for Publication: 4680-2022/CXBIPH/01-66/KHTNVCN.
Decision number for Publication: 81b/QĐ-KHTNCN was issued on 13 December 2022.
Printing and copyright deposit were completed in 4th quarter, 2022.

# NUMERICAL STUDY OF LINEAR OPTICAL PROPERTIES OF $As_2S_3$ GLASS PCF TAKING INTO ACCOUNT THE DIFFERENCE IN STRUCTURAL PARAMETERS

**Tran Tran Bao Le[a], Minh Nguyen Hong[a], Dung Tran Tien[a], Anh Truong Duc[a], Duy Le Pham[a], Phuong Nguyen Thi Hong[b], Luu Mai Van[c], Thuy Do Thanh[a], Lanh Chu Van*[a]**

[a)]Department of Physics, Vinh University, 182 Le Duan, Vinh City, Vietnam
[b)]Nguyen Chi Thanh High School, Hoa Thanh District, Tay Ninh Province, Vietnam
[c)] Hanoi Open University, Nguyen Hien Str., Bach Khoa Ward, Hai Ba Trung Dist., Hanoi, Vietnam

*Email: chuvanlanh@vinhuni.edu.vn

**Abstract**. This work proposes a special hexagonal lattice photonic crystal fiber (PCF) based on $As_2S_3$ glass with a heterogeneous structure in the micro-cladding. The linear optical characteristics of PCF including effective refractive index, chromatic dispersion, and confinement loss have been numerically analyzed over a wide wavelength range. The results show that all dispersion curves possess a zero-dispersion wavelength (ZDW) and it tends to shift towards the long wavelength as the filling factor decreases. Two fibers with a flat dispersion profile and close to the zero-dispersion line are selected as the two optimal structures and then the values of the optical properties are calculated at the corresponding pump wavelength. As a result, our PCFs obtain small dispersion and very low confinement loss. These are well-suited structures for broadband supercontinuum generation (SC) thanks to the support of pump pulses in the anomalous dispersion regime.

**Keywords**: *$As_2S_3$ glass, Linear optical properties, Different air-hole size, Flat dispersion, Low confinement loss, Hexagonal lattice*.

## I. INTRODUCTION

A photonic crystal fiber (PCF) is defined as an optical fiber that uses a photonic crystal to create a cladding around its core. Up to now, a number of studies on PCF have shown that it has many advantages over conventional optical fibers in flexible structure leading to control of characteristic quantities [1-3]. Therefore, PCF has many applications in optical communication such as signal transmission for implanted medical devices, transatlantic submarine cable systems, passive optical devices, optical transmission systems, light propagation, high-sensitivity temperature sensor, eliminating dispersion compensation in long-haul transmission [4, 5]. PCFs are characterized not only by quantities exhibiting nonlinearity, but also by linear optical properties including dispersion, effective refractive index, and loss. Among them, chromatic dispersion is an important factor for telecommunication and nonlinear applications, especially supercontinuum generation (SCG) [6]. In addition, confinement loss is also of great interest in this type of application although PCF has very low loss compared to other fibers used in telecommunication systems. This quantity together with dispersion can be controlled as desired by adjusting the lattice parameters in the cladding of the PCF.

PCFs can be classified into solid core PCFs and hollow-core ones. Several publications on hollow PCF have demonstrated that the use of highly nonlinear liquid to fill the core of PCF significantly improves fiber nonlinearity [7-9]. However, this process is extremely difficult experimentally because the liquid tends to leak during infiltration into the core. Recently, a number of research groups have conducted an in-

**ISBN: 978-604-357-120-2**

depth analysis of the characteristic quantities of solid-core PCFs with common substrates of silica and have achieved some remarkable results such as small and flat dispersion, high nonlinearity and low confinement loss, small effective mode area [10-12]. The fact that silica's nonlinear refractive index is very small and its attenuation is high over the long wavelength range, thus its applications are limited to the 2 μm range. The replacement of chalcogenide glasses has overcome the aforementioned disadvantage of silica. In chalcogenide glass types, $As_2S_3$ is an ideal material due to its nonlinearity of 100-500 times greater than silica and low linear loss [13]. It exhibits strong normal dispersion at telecom wavelengths (1.55μm) [14] and a wide transmission window in the near- and mid-infrared (long wavelength cut-off at 9.4 μm). This is a commercially available glass bulk and has a good fiber-drawing capability [15]. Therefore, it is convenient for experimental investigations such as the deposition of amorphous chalcogenide layers to the development of fiber-based devices combined with sophisticated glasses for supercontinuum generation as well as other nonlinear applications [16]. The high efficiency of using this substrate has been further demonstrated by a recent series of publications [17-19], with uniform air holes facilitating the production and fabrication of PCFs.

In this paper, we introduce a new type of $As_2S_3$-PCF with dissimilar air holes arranged cyclically in a regular hexagonal lattice. By changing the filling factor and lattice constant, we can flexibly control the dispersion curves to select the optimal structures for SCG. Next, the linear optical characteristics of effective refractive index and confinement loss are also optimized along with chromatic dispersion thanks to the difference between the diameters of the first air-hole ring and the remaining rings in the cladding.

## II. NUMERICAL MODELING

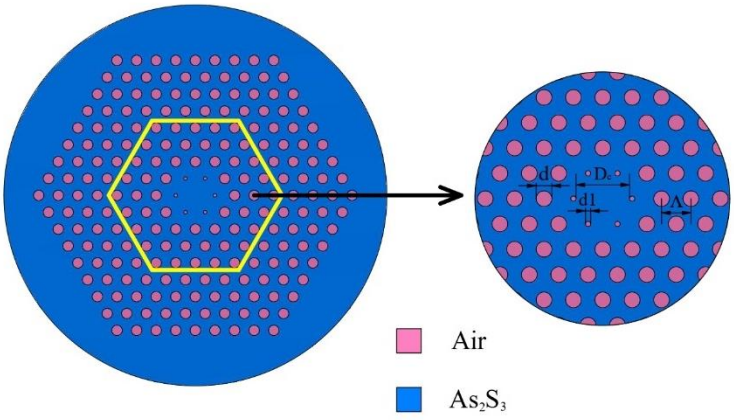


**Fig 1**. *The geometrical structure of PCF with a hexagonal lattice and $As_2S_3$ substrate.*

We used Lumerical Mode Solutions [20] software to design the solid core PCF structure as shown in Fig 1. The blue region is the $As_2S_3$ substrate, while the air is depicted by the yellow area. The lattice consists of eight air-hole rings with diameter *d*



**ISBN: 978-604-357-120-2**

arranged in a regular hexagon with lattice constant $\Lambda$. The linear filling factor is defined as $f = d/\Lambda$. In the numerical simulation, we use lattice constant equal to 1.0 µm and 2.0 µm, and the first ring filling factor $d_1/\Lambda$ change 0.3, 0.35, 0.4, 0.45, 0.5, 0.55, 0.6, 0.65, 0.7, 0.75 and 0.8, respectively. Meanwhile, the filling factor $d/\Lambda$ of other rings is kept constant at 0.95. The core diameter ($D_c$) is determined by the formula $D_c = 2\Lambda - d_1$, where $d_1$ is the diameter of the first ring air holes. Changing the first air-hole diameter affects the dispersion characteristic and the displacement of the zero-dispersion wavelength (ZDW). Whereas, the mode attenuation is determined by the rest, especially for higher modes [21]. The novelty in this model helps us to simultaneously optimize the dispersion and confinement loss characteristics of the fiber.

The real part of the linear refractive index of the $As_2S_3$ material is calculated by the Sellmeier equation as follows [22].

$$n(\lambda) = \sqrt{1 + \sum_{n=1}^{3} \frac{A_n \lambda^2}{\lambda^2 - B_n}} \quad (1)$$

With the Sellmeier coefficients $A_1$ = 1.8983, $A_2$ = 1.9222, $A_3$ = 0.8765 and $B_1$ = 0.0225 µm$^2$, $B_2$ = 0.0625 µm$^2$, $B_3$ = 0.1125 µm$^2$; $\lambda$ in µm. The nonlinear refractive index of $As_2S_3$ is 4.2×10$^{-18}$ m$^2$/W.

## III. LINEAR OPTICAL PROPERTIES OF $As_2S_3$-PCF DESIGN

We calculate the dispersion characteristic in the two cases $\Lambda$ = 1.0 µm and $\Lambda$ = 2.0 µm. Figs. 2 and 3 show the dispersion curves including the region below the zero-dispersion line (normal dispersion) and the part above the zero-dispersion line (anomalous dispersion). In general, we obtain anomalous dispersion with one ZDW and two ZDWs for two lattice constants.

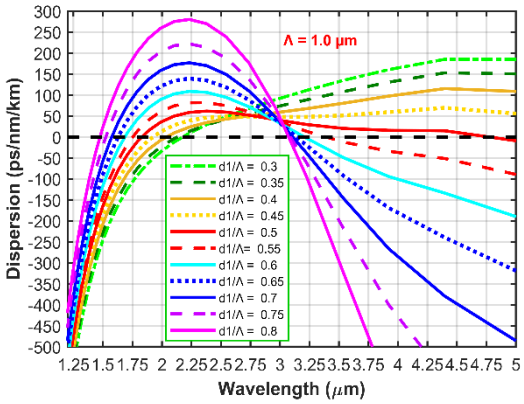


**Fig 2**. *Dispersion properties of $As_2S_3$-based PCF with $\Lambda$ = 1.0 µm.*

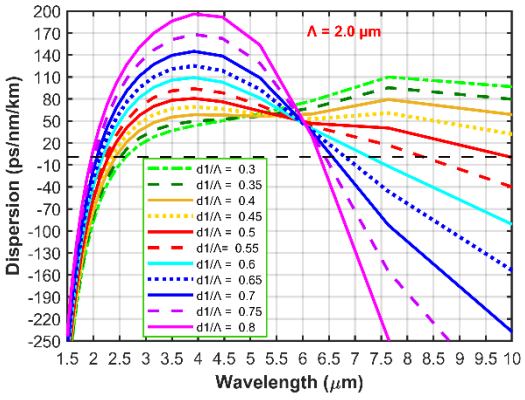


**Fig 3**. *Dispersion properties of $As_2S_3$-based PCF with $\Lambda$ = 2.0 µm.*

With the filling factor from 0.3 to 0.45, the dispersion curves have a small slope, intersecting the zero-dispersion curve at a point, i.e. anomalous dispersion with a ZDW achieved in the investigated wave range. On the other hand, anomalous dispersion with two ZDWs is obtained with a large filling factor; the slope of the dispersion curves is also larger. In particular, the fiber with $d_1/\Lambda$ = 0.45 has a very wide flatness of dispersion in the 1.9-5 µm wavelength range (Fig 2). Obviously, the dispersion changes with varying lattice parameters.

**ISBN: 978-604-357-120-2**

The properties of the dispersion, especially the displacement of the ZDW, are also influenced by the filling factor and the lattice constant as shown in Table 1. When increasing the lattice constant from 1.0 µm to 2.0 µm, the ZDWs begin to shift to longer wavelength regions; this is also observed when decreasing the filling factor value. The difference between the sizes of the air holes in our design makes the light restriction in the core stronger, i.e. the structural parameters play an important role in the adjustment of the dispersion feature. From the above results, we propose two structures with optimal dispersion with $\Lambda$ = 1.0 µm, $d_1/\Lambda$ = 0.45 and $\Lambda$ = 1.0 µm, $d_1/\Lambda$ = 0.5, respectively. They are called #$F_1$, #$F_2$.

**Table 1.** *The wavelength at the zero-dispersion point of PCFs with $\Lambda$ = 1.0 µm and $\Lambda$ = 2.0 µm and $d_1/\Lambda$ varies from 0.3 to 0.8.*

| $d_1/\Lambda$ | $\Lambda$ = 1.0 µm | | $\Lambda$ = 2.0 µm | |
|---|---|---|---|---|
| | ZDW 1 | ZDW 2 | ZDW 1 | ZDW 2 |
| 0.3 | 2.176 | - | 2.606 | - |
| 0.35 | 2.131 | - | 2.506 | - |
| 0.4 | 2.039 | - | 2.416 | - |
| 0.45 | 1.926 | - | 2.349 | - |
| 0.5 | 1.83 | 4.473 | 2.282 | - |
| 0.55 | 1.754 | 3.391 | 2.228 | 8.339 |
| 0.6 | 1.686 | 3.307 | 2.17 | 7.296 |
| 0.65 | 1.628 | 3.141 | 2.115 | 6.823 |
| 0.7 | 1.575 | 3.108 | 2.065 | 6.578 |
| 0.75 | 1.525 | 3.088 | 2.013 | 6.434 |
| 0.8 | 1.475 | 3.073 | 1.961 | 6.33 |

Fig 4 shows the dispersion characteristics of the proposed PCFs. #$F_1$ fiber has a flat anomalous dispersion curve and the value of ZDW is 1.926 µm, while fiber #$F_2$ has two ZDWs at 1.83 µm and 4.473 µm. The center wavelength of the input pulse (the pump wavelength) chosen for fibers #$F_1$ and #$F_2$ is 2.0 µm and 2.5 µm, respectively. The structural parameters of the proposed fibers and their dispersion values at the pump wavelength are presented in Table 2.



**ISBN: 978-604-357-120-2**

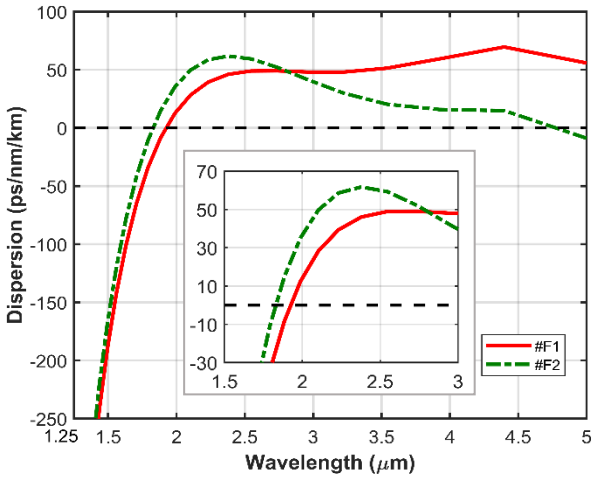


**Fig 4**. *The dispersion properties of proposed PCFs.*

The effective refractive index of PCFs is affected by the variation of wavelength and lattice parameters (Fig 5). As observed, the real part of the effective refractive index $n_{eff}$ of the PCFs decreases with increasing wavelength. The $n_{eff}$ curves of the #$F_1$ and #$F_2$ are quite close, in which the effective refractive index of #$F_1$ is slightly higher than that of #$F_2$. Fig 6 studies the confinement loss characteristics of two optimal fibers. The confinement loss curves almost coincide with the horizontal axis in the wavelength region of less than 4.4 µm. The longer the wavelengths are, the more separate the curves are and the magnitude of $L_c$ decreases in the case of increasing core diameter because of the increase of the real part of the effective refractive index. In other words, $L_c$ depends on the imaginary part of $n_{eff}$ according to the formula [11].

$$L_c = 8.686 k_0 \,\mathrm{Im}\left(n_{eff}\right) \mathrm{q} \qquad (2)$$

with Im[$n_{eff}$] represents the imaginary part of the effective refractive index [21], $k_0$ is the number of waves in free space. Table 3 illustrates the confinement loss value for the designs at the pump wavelength. At 2.0 µm and 2.5 µm pumping wavelengths, there was no significant difference in the $L_c$ values of both fibers.

**Table 2.** *The dispersion value of #$F_1$ and #$F_2$ at the pump wavelength. The dispersion in ps.[nm.km]$^{-1}$*

| # | $\Lambda$ (µm) | $d_1/\Lambda$ | *The pump wavelength* (µm) | $D$ (ps.[nm.km]$^{-1}$) |
|---|---|---|---|---|
| #$F_1$ | 1.0 | 0.45 | 2.0 | 14.061 |
| #$F_2$ | 1.0 | 0.5 | 2.5 | 48.131 |

**ISBN: 978-604-357-120-2**

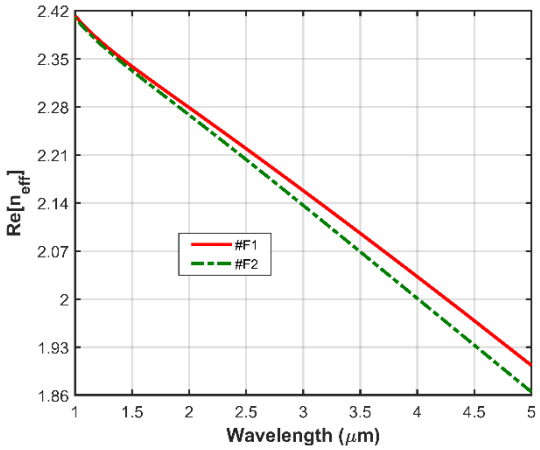


**Fig 5**. *The effective refractive properties of proposed PCFs.*

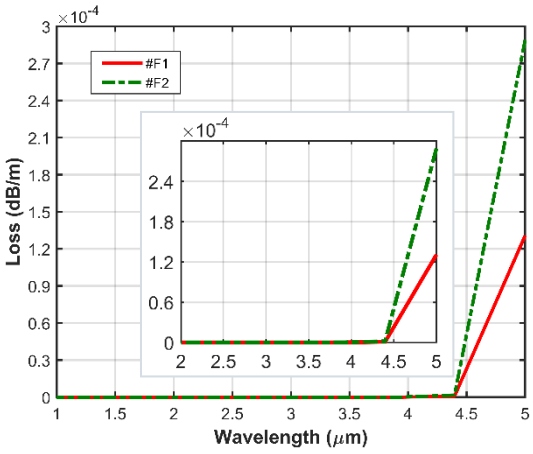


**Fig 6**. *The confinement loss properties of proposed PCFs.*

**Table 3.** *The effective refractive index and the confinement loss value of the optimal structure at the pump wavelength.*

| # | $D_c$ (μm) | *The pump wavelength* (μm) | $n_{eff}$ | $L_c$ (dB/m) |
|---|---|---|---|---|
| $\#F_1$ | 1.46 | 2.0 | 2.279 | $-1.12\times10^{-18}$ |
| $\#F_2$ | 1.4 | 2.5 | 2.203 | $-1.44\times10^{-18}$ |

Comparing studies [11, 23, 24] in Table 4, we find that our work has smaller dispersion and lower confinement loss. This has confirmed the effectiveness of numerical model innovation in controlling and optimizing the linear optical properties of the fiber.

**Table 4.** *The dispersion and confinement loss values of proposed PCFs compared with previous publications.*

| Material | References | $D_c$ (μm) | *The pump wavelength* (μm) | $D$ (ps.[nm.km]$^{-1}$) | $L_c$ (dB/m) |
|---|---|---|---|---|---|
| $As_2S_3$ | $\#F_1$, this work | 1.46 | 2.0 | 14.061 | $-1.12\times10^{-18}$ |
| $As_2S_3$ | $\#F_2$, this work | 1.4 | 2.5 | 48.131 | $-1.44\times10^{-18}$ |
| Silica | [23] | 1.54 | 1.55 | 103.5 | $5.97\times10^{-7}$ |
| Tellurite | [11] | 1.2 | Three telecommunication windows | The order of $10^6$ | The order of $10^{-8}$ |
| $Ge_{11.5}As_{24}Se_{645}$ | [24] | 2.0 | 2.306-6.52 | 71.42 | $2.3\times10^{-10}$ |



**ISBN: 978-604-357-120-2**

## IV. CONCLUSION

A new design of hexagonal lattice PCF with $As_2S_3$ glass substrate was designed and linear optical properties such as confinement loss, effective refractive index, and chromatic dispersion were numerically analyzed. After many simulations are performed, we obtain ZDW-existence flat anomalous dispersion curves that facilitate optimization of the linear characteristics of the fibers. The first structure with $\Lambda$ = 1.0 µm, $d_1/\Lambda$ = 0.45 has the dispersion and confinement loss at the 2.0 µm pump wavelength of 14.061 ps[nm.km]$^{-1}$ and $1.12\times10^{-18}$ dB/m, respectively. Meanwhile, these values for the second fiber are 48.131 ps[nm.km]$^{-1}$ and $-1.44\times10^{-18}$ dB/m at 2.5 µm ($\Lambda$ = 1.0 µm, $d_1/\Lambda$ = 0.5). The reason for achieving flat and small dispersion along with low confinement loss at the same time is the difference in air-hole diameters between lattice rings. The proposed fibers find potential applications in mid-infrared SCG.

## ACKNOWLEDGMENTS

This research was funded by Vietnam National Foundation for Science and Technology Development (NAFOSTED) under grant number 103.03-2020.03 and Vingroup JSC and supported by the Master, PhD Scholarship Programme of Vingroup Innovation Foundation (VINIF), Institute of Big Data, code [VINIF.2021.TS.155].

## REFERENCES

[1] J. C. Knight, T. A. Birks, P. St. J. Russell, and D. M. Atkin, *Opt. Lett.* Vol. **21**, 1996, pp. 1547-1549.

[2] T. A. Birks. J. C. Knight, and P. S. J. Russell, *Opt. Lett.* Vol. **22**, 1997, pp. 961-963.

[3] R. F. Cregan. B. J. Mangan. J. C. Knight. T. A. Birks. P. S. J. Russell. P. J. Roberts, and D. C. Allan, *Science*. Vol. **285**, 1999, pp. 1537-1539.

[4] M. F. H. Arif, M. J. H. Biddut, M. S. I. Babu, H. M. M. Rahman, M. M. Rahman, B. Jahan, M. S. Chaity, and S. M. Khaled, *Opt. Photon. J*. Vol. **7**, 2017, pp. 221-234.

[5] M. F. H. Arif, K. Ahmed, S. Asaduzzaman, and M. A. K. Azad, *Photon. Sens*. Vol. **6**, 2016, pp. 279-288.

[6] C. V. Lanh, N. T. Thuy, L. T. B. Tran, H. T. Duc, V. T. M. Ngoc, L. V. Hieu, and H. V. Thuy, *Photon. Nanostruct. Fundam. Appl*. Vol. **48**, 2022, pp. 100986(1-10).

[7] C. V. Lanh, N. T. Thuy, H. T. Duc, L. T. B. Tran, V. T. M. Ngoc, D. V. Trong, L. C. Trung, H. D. Quang, and D. Q. Khoa, *Opt. Quant. Electron*. Vol. **54**, 2022, pp. 300(1-17).

[8] H. Q. Quy and C. V. Lanh, *Indian J. Pure Appl. Phys.* Vol. **59**, 2021, pp. 522-527.

[9] B. Wan, L. Zhu, X. Ma, T. Li, and J. Zhang, *Sensors*. Vol. **21**, 2021, pp. 284(1-18).

[10] L. T. B. Tran, N. T. Thuy, V. T. M. Ngoc, L. C. Trung, L. V. Minh, C. L. Van, D. X. Khoa, and C. V. Lanh, *Photon. Lett. Poland*. Vol. **12**, 2020, pp. 106-108.

[11] S. Luke, S. K. Sudheer, and V. P. M. Pillai, *Optik*, Vol. **127**, 2016, pp. 11138-11142.

[12] D. V. Trong, L. T. B. Tran, N. T. Thuy, V. T. M. Ngoc, T. D. Tan, C. V. Lanh, H. T. Duc, and N. T. Thuy, *Proc. The 7th Academic Conf. on Natural Science for Young Scientists, Master and PhD. Students from Asean Countries*. Ha Noi & Vinh City, Vietnam, 2021, pp. 293-300.

[13] C. Xiong, E. Magi, F. Luan, A. Tuniz, S. Dekker, J. S. Sanghera, L. B. Shaw, I. D. Aggarwal, and B. J. Eggleton, *Appl. Opt.* Vol. **48**, 2009, 5467-5474.

**ISBN: 978-604-357-120-2**

[14] M. R. E. Lamont, C. M. de Sterke, and B. J. Eggleton, *Opt. Express*. Vol. **15**, 2007, pp. 9458–9463.
[15] C. Markos, *Sci. Rep*. Vol. **6**, 2016, pp. 31711(1-8).
[16] C. Markos, S. N. Yannopoulos, and K. Vlachos, *Opt. Express*. Vol. **20**, 2012, pp. 14814–14824.
[17] K. F. Fiaboe, S. Singh, R. Rai, and P. Kumar, *J. Emerg. Technol. Innovat. Res*. Vol. **6**, 2019, pp. 280-285.
[18] AKM S. J. Choyon and R. Chowdhury, *Optik*. Vol. **258**, 2022, pp. 168857(1-11).
[19] T. Peng, T. Xu, and X. Wang, *IEEE Access*. Vol. **5**, 2017, pp. 17240-17245.
[20] https://www.lumerical.com/products/mode
[21] K. Saitoh, M. Koshiba, T. Hasegawa, and E. Sasaoka, *Opt. Express*. Vol. **11**, 2003, pp. 843(1-10).
[22] E. C. Magi, D. I. Yeom, H. C. Nguyen, M. R. E. Lamont, D. I. Yeom, and B. J. Eggleton, *Opt. Express*. Vol. **15**, 2007, pp. 10324-10329.
[23] G. D. Krishna, V. P. M. Pillai, and K. G. Gopchandran, *Opt. Fiber Technol*. Vol. **51**, 2019, pp. 17-24.
[24] M. Z. Alam, M. I. Tahmid, S. T. Mouna, M. A. Islam, and M. S. Alam, *Opt. Communic*. Vol. **500**, 2021, pp. 127322(1-10).



**ISBN: 978-604-357-120-2**